Molecular Electrostatics for Exploring Complexes of Carbonyl Compounds and Hydrogen Fluoride

Shridhar R. Gadre* and Pravin K. Bhadane

Department of Chemistry, University of Pune, Pune 411 007, India

Received: November 30, 1998

The negative-valued molecular electrostatic potential (MESP) minima (V_{min}) observed in the substituted carbonyl molecules are found to be a sensitive measure for the analysis of the electronic charge perturbations due to the substituents. MESP topography of eight monosubstituted aliphatic carbonyl molecules (HCOR: R = H, F, Cl, CN, OH, SH, NH_2, CH_3, CF_3, NO_2) [following Bobadova-Parvanova, P.; Galabov, B. *J. Phys. Chem. A* **1998**, *102*, 1815] is carried out at the HF-SCF/6-31G** level for assessing this scheme. The V_{min} values are seen to clearly reflect the changes due to the electron donating/withdrawing substituents. The electrostatic potential for intermolecular complexation (EPIC) model is used for predicting the possible hydrogen-bonded structures of the carbonyl molecules with the hydrogen fluoride. These complexes are further optimized at the HF-SCF/6-31G** level of theory. An excellent linear correlation is obtained with EPIC energy and the corresponding optimized interaction energy of the complex. Total correction to the ab initio SCF interaction energy due to basis set superposition error and zero-point energy is found to be about 40% of the SCF interaction energy. The HF molecule binds from the nonsubstituted sides of the HCOR molecules for R═H, F, Cl, CN, and CF_3. On the other hand, it is seen to bind from the substituted side for R═OH, SH, NH_2, and CH_3. The effect of substitution on the charge distribution and on hydrogen bonding is discussed.

I. Introduction

Interactions of the carbonyl group are important in chemistry because the group is common in many molecules of biological interest,[1] particularly carbohydrates.[2] Both the aromatic and aliphatic carbonyl molecules are extensively used in the pharmaceutical industry.[3] The aliphatic carbonyl molecules, viz., aldehydes and ketones, are found to occur widely in nature and used in many manufactured products. For example, ants use the formic acid as a poison and inject it when they bite their victims. It is also used as a grain preservative and in soaps. Similarly, formaldehyde is used as a solvent to control biological degradation and its polymers are used in manufacturing high-strength plastics. By considering these wide variety of applications, attempts have been made to understand the nature of the carbonyl bond,[4] C═O, of carbonyl molecules and its interaction with the acid molecule.[5−7] These studies reveal that the polarity of the C═O group has a big influence on the intrinsic properties of carbonyl compounds, but it has less effect on the extrinsic properties such as intermolecular interactions.

The molecular structure of the weakly bound complexes can be determined from the rotational or vibrational spectra of the molecule.[8] They can also be predicted by applying computational tools based on rigorous quantum mechanical methods[9] or employing simplified theoretical models.[10,11] Molecular properties such as the molecular electron density and the electrostatic potential (MESP) are closely connected with molecular structure. Utilization of these properties for a particular series of molecules is expected to provide insights into what governs their intermolecular interactions.

In recent years, MESP has attracted much attention as a meaningful descriptor of molecular reactivity,[12] physical properties[13] of the molecule, and intermolecular interactions.[14] Haeberlein and Brinck[15] have recently analyzed the substituent effects in para-substituted phenoxide ions and found a close relation between the minima of the electrostatic potential observed near the phenoxide oxygen and the gas-phase acidities. In a recent work,[16] Gadre et al. have found the existence of a good linear correlation between the minimum MESP values observed over the benzene ring near the para and meta carbons with the corresponding Hammett constants. This work showed that a result of the electronic effects of a substituent is vividly brought out by MESP. Recently, they have also used the MESP to probe the cation binding patterns of hydrocarbon molecules.[17]

In various electrostatic models for the investigation of vdWs (van der Waals) complexes, MESP has been used as a key parameter for the calculation of the interaction energy.[10a] In this connection, Gadre et al. have developed an MESP topography-based model, electrostatic potential for intermolecular complexation (EPIC), for the investigation of weakly bound molecular complexes.[18] They have successfully used it for the investigation of the dimers[19] and trimers[20] of the DNA bases. In the present work, we consider some substituted aldehyde molecules toward an MESP topographical investigation and their interaction with a model test proton donor, the hydrogen fluoride molecule. In a recent work,[21] Bobadova-Parvanova and Galabov have correlated the MESP at the electronegative oxygen atom of a series of carbonyl molecules with the hydrogen bond energies of carbonyl−hydrogen fluoride bimolecular complexes. However, their investigation is limited to MESP at the carbonyl oxygen nucleus and to only one stable structure. The present work utilizes a newly developed EPIC[18] model for the prediction of hydrogen-bonded structure and energy. Here, we explore almost all the possible stable structures as predicted by MESP topography and the EPIC model. A correlation of the ab initio interaction energy with the EPIC interaction energy is also presented.

10.1021/jp984541a CCC: $18.00
Published on Web 04/21/1999

II. Methodology

The utilization of molecular electrostatic potential (MESP)[22] is now very common in the study of molecular interactions because of its clearness and ease of application.

The molecular electrostatic potential (MESP), V, at a point $\mathbf{r}$ is defined as

$$V(\mathbf{r}) = \sum_{A} \frac{Z_A}{|\mathbf{R}_A - \mathbf{r}|} - \int \frac{\rho(\mathbf{r}')}{|\mathbf{r}' - \mathbf{r}|} d^3\mathbf{r}' \quad (1)$$

where $\{Z_A\}$ are charges of nuclei situated at $\{\mathbf{R}_A\}$ and $\rho(\mathbf{r})$ denotes the molecular electron charge density. The right-hand side of eq 1 suggests that $V(\mathbf{r})$ is negative in the electron-dominated regions and thus directly provides information regarding the electron-rich sites. Equation 1 also suggests that the $V(\mathbf{r})$ may be endowed with rich topographical features. The topographical analysis[23] of $V(\mathbf{r})$ is based on locating and characterizing the critical points (CP's), viz., the points at which $\nabla V(\mathbf{r}) = 0$, and its characterization is done by calculating the number of nonzero eigenvalues of the Hessian matrix $\mathbf{A}$, the elements of which are defined by

$$A_{ij} = \frac{\partial^2 V(\mathbf{r})}{\partial x_i \partial x_j}|_{\mathbf{r}=\mathbf{r}_c} \quad (2)$$

where $\mathbf{r}_c$ is a critical point. A nondegenerate minimum is always characterized by three eigenvalues of the Hessian.[24] In the present study, we have considered only negative-valued minima (all the eigenvalues are positive) and saddles (one of the eigenvalue is negative) for the initial positioning of the carbonyl and HF molecule in the guess geometry of the complex. The guess geometry of the complex and the potential-derived atomic charges are the inputs to the EPIC model. The EPIC model evaluates MESP at the atom centers and optimizes the complex by minimizing the electrostatic interaction energy, E_{EPIC},

$$E_{EPIC} = \frac{1}{2}\{\sum V_{A,i} q_{B,i} + \sum V_{B,i} q_{A,i}\} \quad (3)$$

where V is the MESP of one species evaluated at the ith atomic site of the other species where the potential-derived charge is q. Use of vdWs radii of heavy atoms and appropriately scaled hydrogen radius prevents the collapse of the two species.

The EPIC optimized structure of the complex is further optimized at the ab initio HF-SCF/ 6-31G** level of theory. Intermolecular interaction energy of the complex formed by A and B molecules is[26]

$$\Delta E_{SCF} = E_{AB}^{\alpha\cup\beta}(AB) - E_{A}^{\alpha}(A) - E_{B}^{\beta}(B) \quad (4)$$

where $E_{AB}^{\alpha\cup\beta}(AB)$, $E_{A}^{\alpha}(A)$, and $E_{B}^{\beta}(B)$ are the total energies of the fully optimized complex AB, monomer A, and monomer B, respectively. Equation 4 overestimates the intermolecular interaction energy owing to the basis set superposition error (BSSE) and zero-point energy error. The BSSE correction can be estimated using the function counterpoise (fCP)[25] technique, and the corrected ΔE_{SCF} is

$$\Delta E_{FCP} = E_{AB}^{\alpha\cup\beta}(AB) - E_{AB}^{\alpha\cup\beta}(A) - E_{AB}^{\alpha\cup\beta}(B) \quad (5)$$

where $E_{AB}^{\alpha\cup\beta}(A)$ and $E_{AB}^{\alpha\cup\beta}(B)$ are the energies of monomers A and B, respectively, evaluated at the geometry of complex AB using a full basis set.

Equations 4 and 5 will not converge to the same result, since the energies of A and B are calculated at different geometries. This problem can be overcome by estimating the interaction energy proposed by Xantheas:[26]

$$\Delta E_{BSSE} = E_{AB}^{\alpha\cup\beta}(AB) - E_{AB}^{\alpha\cup\beta}(A) - E_{AB}^{\alpha\cup\beta}(B) + E_{rel}^{\alpha}(A) + E_{rel}^{\beta}(B) \quad (6)$$

where

$$E_{rel}^{\alpha}(A) = E_{AB}^{\alpha}(A) - E_{A}^{\alpha}(A)$$

and

$$E_{rel}^{\beta}(B) = E_{AB}^{\beta}(B) - E_{B}^{\beta}(B) \quad (7)$$

are the relaxation energies of the A and B fragments of the AB complex, respectively.

The geometries of carbonyl compounds and their hydrogen-bonded complexes with the HF molecule are optimized at the ab initio HF/6-31G** level using the GAMESS[27] package. The $\rho(\mathbf{r})$ [see eq 1] is computed from the quantum mechanical ab initio wave functions. These wave functions of carbonyl compounds and HF molecules are calculated using the UNIMOL[28] package at the 6-31G** basis set level. The UNIPROP[29] and GRID[30] programs are used respectively to carry out topographical analysis of MESP and to obtain the MESP-derived atom-centered charges for the carbonyl compounds and HF molecule.

III. Results and Discussion

MESP CPs of the carbonyl molecules and the optimized structures of the hydrogen-bonded complexes of the HCO-R···HF (R = H, F, Cl, CN, OH, SH, NH_2, CH_3, CF_3, NO_2) series of molecules are shown in Figure 1. The EPIC model geometries are found to be nearly similar to the corresponding fully optimized ab initio one. The typical hydrogen bond distances obtained from the EPIC model are found to be 0.3−0.5 Å less than the corresponding ab initio ones, which is an artifact of the radii used for exclusion purposes. It has been noted that the EPIC model energy, E_{EPIC}, is found to be 5−10% less than the corresponding ab initio one. These observations show that the EPIC model provides a good estimate of the geometry of the complex, which can be further optimized using the ab initio HF-SCF method. It implies that the relative orientation of two monomers in the complex is mainly controlled by the electrostatic "push−pull" forces acting between the different regions of the monomers. All the carbonyl MESP CPs of interest are found to be in the molecular plane and are negative-valued nondegenerate ones. In Figure 1, M1 and M2 denote (3, +3) CP's, i.e., minima, and S1 represents a (3, +1) saddle. The EPIC model energy, E_{EPIC} (cf. eq 3), and the fully optimized ab initio HF-SCF interaction energy, i.e., energy of the hydrogen bond formation calculated as the difference between the respective SCF energies of the complex and the monomers, ΔE_{SCF}, are given in Table 2. MESP at the negative-valued CPs (M1, M2, S1) and the CP positions from the carbonyl oxygen atom are reported in Table 1.

An examination of Table 1 reveals that on substitution of an electronegative group the carbonyl CP that is in the vicinity of the substituent acquires a more negative MESP value. However, the corresponding H-bonded structure is found to be less stable (cf. Table 2, for example, structure **L2** in Figure 1b). On the other hand, substitution of the hydroxyl and amine groups exactly does the reverse. The effect of substitution is observed

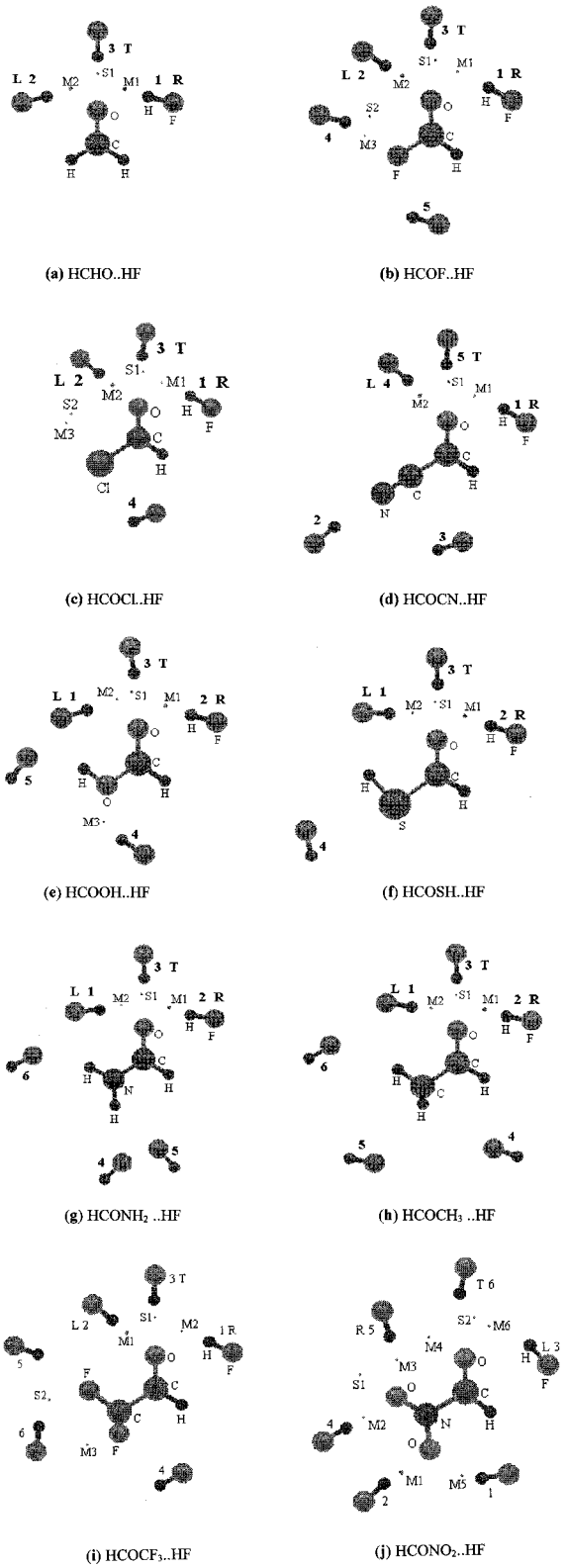

Figure 1. Various sites of the hydrogen bonding of HCOR···HF complexes (R = H, F, Cl, CN, OH, SH, NH_2, CH_3, CF_3, NO_2). M1−M6, S1, and S2 are the MESP critical points (CP) of HCOR. See text for details.

to be maximum for the HCOOH···HF complex. Here, the large difference in MESP at M1 and M2 and the shift of their angular positions (cf. Table 1) are indicative of a substantial variation in the charge distribution of the C═O region. Structure **1** is found to be more stable because of the double H-bond. However, the MESP values at M1 and M2 (cf. Table 1) suggest that an approaching monatomic cation such as Li^+ will prefer the M1 (most negative) side of this molecule. The salient features of the MESP topography of the carbonyl molecules along with the structural features and interaction energies at the SCF level of the hydrogen-bonded HCOR···HF complexes are discussed below. Energy corrections due to zero-point energy, basis set superposition error (BSSE), and fragment relaxation are taken up later.

(A) HCHO···HF. Figure 1a shows the MESP CPs of the HCHO molecule. The symmetrical lone pair minima M1 and M2 located at a distance 1.23 Å from the oxygen atom appear at the lone pair position of oxygen atom (cf. Table 1). Their location suggests that there is greater electron density over the more electronegative oxygen atom. The saddle, S1, found on the C_2 axis of the molecule is located at a distance of 1.3 Å from O. The locations of M1, M2, and S1 are found near the H atom of the HF of the H-bonded structures **1**, **2**, and **3**, respectively. As can be seen from the Figure 1a, structures **1** and **2** are nonlinear (∠COH, 105.4°; ∠OHF, 151.15°). These angles are found to be nearly equal to that of the experimentally estimated[5] ones (115°, 163°). The experimental O···H bond length (1.79 Å)[5] is in reasonable agreement with the theoretically calculated (1.86 Å) value. It is interesting to note that the angles ∠COM1 and ∠OM1H are found to be nearly equal to 120°, and the angle between M1 and H−F is indeed very small (5.4°). Structure **3** appears on the C_2 axis at a distance $R_{O\cdots H}$ of 1.91 Å, and ΔE_{SCF} is −26.29 kJ mol^{-1}. These angles show that direction of the H−F molecule can be predicted from the location of CPs. The two symmetrical structures **1** and **2** are found to be the most stable structures (cf. Table 2). It is noteworthy that the F atom in HF is tilted toward H of HCHO, as was shown by the celebrated Buckingham−Fowler[10a] model. In fact, this success was one of the factors leading to the wide acceptability of this model.

(B) HCOOH···HF and HCOSH···HF. The C═O and O−H groups of the formic acid are so close that they perturb the charge distribution of each other. As expected, the location and value of MESP at the CPs of this molecule are significantly different from the symmetrically charge-distributed HCHO one (Table 1). The CPs M1 and M2 are located almost at the same distance from O; however, the angle ∠COM2 is larger by 15° than the ∠COM1. The saddle S1 is turned toward the hydroxyl group by 10°, and it is closer to carbonyl O than the S1 of HCHO one. The H-bonded structures of this complex are displayed in Figure 1e. The structure on the left (**L**) is found to be the most stable one with E_{EPIC} and ΔE_{SCF} values of −44.05 and −49.15 kJ mol^{-1}, respectively. The extra stability of **1** is due to the two H-bonds (C═O···H and O−H···F) between the two molecules. The ΔE_{SCF} of **3** (−28.41 kJ mol^{-1}, $R_{O\cdots H}$ = 1.9 Å) is comparable to those of **1** and **2**, and it makes an angle of 15° with S1. Structure **4** is found near the CP M3 of the MESP value of −120.7 kJ mol^{-1}, which is much less compared to the MESP at M1 and M2. As expected, ΔE_{SCF} (−19.37, $R_{O\cdots H}$ = 1.96 Å) is also less than those of structures **1** and **2**. In the last structure, **5**, formic acid is a proton donor; however, ΔE_{SCF} (−21.05, $R_{H\cdots F}$ = 1.96 Å) is found to be much less compared to others.

The MESP topography and the parameters of the H-bonded structures of HCOSH···HF are expected to be similar to that of the HCOOH···HF system. However, owing to the relatively smaller polarity of the SH group and its nonplanar charge distribution, as indicated by MESP topography (not shown in Figure 1f), the charge distribution in the C═O region remains nearly symmetrical. As expected, the structures on the **L** and

TABLE 1: MESP Topography of Carbonyl Compounds[a]

molecule	V_{M1}	V_{M2}	V_{S1}	R_{M1}	R_{M2}	R_{S1}	∠COM1	∠COM2	∠COS1
HCHO	−202.54	−202.54	−179.27	1.23	1.23	1.30	129.3	129.3	0.0
HCOF	−153.34	−166.56	−146.28	1.33	1.28	1.37	137.2	131.6	6.8
HCOCl	−131.41	−146.36	−124.85	1.30	1.30	1.36	137.0	131.5	7.4
HCOOH	−209.31	−186.15	−183.35	1.23	1.25	1.25	129.5	144.8	9.4
HCOSH	−182.48	−171.28	−161.58	1.25	1.25	1.31	130.9	138.5	2.6
HCOCN	−119.08	−123.02	−105.71	1.29	1.30	1.37	133.2	133.1	2.1
$HCONH_2$	−262.30	−257.05	−243.94	1.20	1.20	1.26	129.3	133.6	4.9
$HCOCH_3$	−227.15	−220.86	−200.13	1.22	1.22	1.29	127.7	130.7	1.2
$HCOCF_3$	−146.02	−140.91	−125.40	1.29	1.28	1.35	130.7	132.1	0.4
$HCONO_2$	−144.39	−143.18	−96.01	4.45	3.96	2.21	37.8	61.5	83.1

[a] M1, M2, and S1 are the minima and saddle points. V_{M1}, V_{M2}, and V_{S1} are the MESP at M1, M2, and S1 points, respectively. R_{M1}, R_{M2}, and R_{S1} are the distances between carbonyl oxygen atom and M1, M2, and S1, respectively (MESP in kJ mol^{-1} and distances in Å).

TABLE 2: Geometrical and Energy Parameters for Carbonyl···HF Complexes[a]

complex	E_{EPIC} (**1**)	E_{EPIC} (**2**)	ΔE_{SCF} (**1**)	ΔE_{SCF} (**2**)	$R_{O\cdots H}$ (**1**)	$R_{CP\cdots H}$ (**1**)	∠COH (**1**)	∠OHF (**1**)
HCHO···HF	−27.59	−27.59	−33.82	−33.82	1.86	0.89	105.4	151.2
HCOF···HF	−23.98	−21.06	−27.94	−24.09	1.98	1.17	102.2	138.8
HCOCl···HF	−21.26	−17.51	−25.93	−21.13	1.99	1.19	101.8	138.1
HCOOH···HF	−44.05	−32.26	−49.15	−35.14	1.85	1.08	110.4	143.3
HCOSH···HF	−31.86	−28.70	−36.34	−32.18	1.86	0.79	119.5	153.5
HCOCN···HF	−20.07	−14.85	−26.26	−17.69	2.01	1.12	102.3	136.4
$HCONH_2$···HF	−50.80	−40.61	−54.99	−45.79	1.76	0.80	110.7	154.7
$HCOCH_3$···HF	−34.17	−32.94	−39.90	−37.94	1.82	0.69	117.5	162.0
$HCOCF_3$···HF	−22.14	−16.29	−27.09	−21.48	1.96	1.05	103.0	150.2
$HCONO_2$···HF	−24.76	−17.13	−29.26	−21.40	4.15	2.72	10.2	89.3

[a] E_{EPIC} and ΔE_{SCF} denotes the EPIC model and fully optimized ab initio interaction energies, respectively. **1** and **2** refer to structures in Figure 1. $R_{O\cdots H}$ is the distance between the carbonyl oxygen and hydrogen of HF of ab initio optimized structure **1**. $R_{CP\cdots H}$ is the distance between the hydrogen of HF and the nearest CP (M1 or M2) of the carbonyl molecule. ∠COH is the angle between C═O and the H atom of HF. ∠OHF is the angle between H−F and the carbonyl oxygen. (Energy in kJ mol^{-1}, distances in Å, and angles in degrees).

R sides are equally stable with a small energy barrier of 4 kJ mol^{-1}, and its most stable structure, **1,** has much less energy compared to that of **1** of the HCOOH···HF (cf. Table 2). The other possible structures, **3** and **4**, have interaction energies of −24.97 and −8.8 kJ mol^{-1}, respectively.

(C) $HCONH_2$···HF, $HCOCH_3$···HF, $HCOCF_3$···HF, and $HCONO_2$···HF. Figure 1g shows the MESP CPs of formamide molecule. MESP value at the CPs suggest a stronger interaction with the electrophile at these sites (cf. Table 1). The double H-bonded structure on the NH_2 side, **L**, is more stable than the **R** one by 9 kJ mol^{-1}. This extra stability is nearly equal to the ΔE_{SCF} of the H···F hydrogen bond structure **4**, found in the vicinity of **1**. The energy of other F-bonded (H···F) structures, **5** and **6** (ΔE_{SCF}: −15.6, −14.4 kJ mol^{-1}) and their orientation with reference to the H atom of N−H are found to be similar to those of **4**. The H bond length of F-bonded structures **4**−**6** is about 0.5 Å more than the H-bonded ones. In general it suggests that the binding of the formamide molecule with HF is stronger than that of HCHO. If the amine group of this complex is replaced by NO_2, then the geometrical and energetic features of the structures are significantly modified as seen from Figure 1j. The structures with HF positions near the NO_2 group are found to be more stable than the C═O···HF one. This is expected because the most negative-valued MESP CPs lie in the vicinity of the NO_2 group.

The MESP CPs of the $HCOCH_3$ are depicted in Figure 1h. The MESP at M1 and M2 are nearly the same. As expected, the energies of the corresponding H-bonded structures are also comparable, the values being −39.90 and −37.94 kJ mol^{-1} respectively. Structure **3** has ΔE_{SCF} and $R_{O\cdots H}$ of −29.89 kJ mol^{-1} and 1.88 Å, respectively. In **4**−**6**, the F atom binds to the methyl group with relatively less interaction energy. It is interesting to compare these features with the results of the $HCOCF_3$···HF complex that are presented in Tables 1 and 2. Comparison of Figure 1h and 1i shows that the binding sites of HF are same in both the complexes; however, the energy ranking of the structures is different.

(D) HCOCN···HF, HCOF···HF, and HCOCl···HF. Here, the carbonyl group is polar with a considerable partial positive charge on the C atom, which is the effect of the electron-withdrawing group attached to it. As expected, a partial negative charge on the N atom increases and more electronic charge is accumulated on the top of the N atom. This charge concentration is indicated by the CP M3 (−117.28 kJ mol^{-1}) for HCOCN that appears at a distance of 1.31 Å from the N atom. The H-bonded structure (N···H) found near the N atom appears to be more stable than structure **L** (−22.57 kJ mol^{-1}). However, structure **R** turns out to be more stable than these two structures, possibly owing to the two H-bonds (O···H and F···H) between the two molecules. In HCOF and HCOCl molecules, the F and Cl atoms carry more negative charge in comparison to the H in HCHO. Thus, the structure on the **L** side is less stable than the **R** one, owing to the repulsion between two electronegative atoms as indicated by parts b and c of Figure 1. The energy of **3** is found to be comparable with that of **1** and **2**. However, structure **4** is less stable than **1** and **2**.

To assess the efficacy of the EPIC model for predicting the complexation energies, a plot of E_{EPIC} versus ΔE_{SCF} is made and shown in Figure 2. The nature of this plot suggests that the qualitative information about the geometry and energy of the hydrogen-bonded complex can be obtained from the EPIC model. The correlation coefficient value of 0.9969 indicates that the EPIC model can be used for a variety of complexes as a predictive tool for obtaining estimates of ab initio interaction energies.

Interaction Energy Decomposition Analysis. The stability of the hydrogen-bonded complex is mainly dependent on the electrostatic interaction between its monomers. It is observed that this interaction is always attractive for the stabilized complex. Other phenomena such as polarization and charge

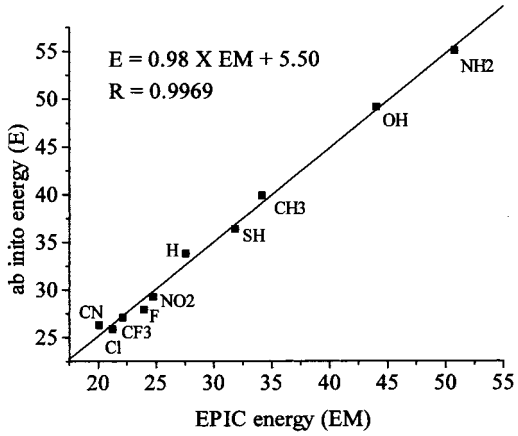

Figure 2. Plot of numerical values of EPIC interaction energy, EM (E_{EPIC}), verses ab initio interaction energy, E (ΔE_{SCF}), of the HCOR···HF complexes (R = CN, Cl, F, H, SH, CH_3, OH, NH_2, CF_3, NO_2).

TABLE 3: Interaction Energy (ΔE_{SCF}) Decomposition Analysis Using the Morokuma and Kitaura (KM) Method for the Structures of HCOOH···HF Complex[a]

structure	ES	PL	CT	ER
1	−68.12	−8.86	−22.72	54.47
2	−46.54	−5.63	−13.65	31.29
3	−27.55	−3.23	−9.87	21.38
4	−27.80	−3.11	−9.91	17.74
5	−19.87	−1.55	−9.91	11.69

[a] ES, PL, CT, and ER are the electrostatic, polarization, charge transfer, and exchange repulsion energy contributions to the total interaction energy, respectively (energy in kJ mol^{-1}).

transfer also take part in the stabilization process. The interaction energy decomposition analysis (EDA) provides details of the various factors involved in the stabilization of the complex. We have performed decomposition analysis according to Morokuma and Kitaura[31] (KM) for this purpose. It gives the details of the energy contribution from electrostatic (ES), polarization (PS), charge transfer (CT), and exchange repulsion (ER) terms. Table 3 presents the EDA for the various structures of HCOOH···HF complex. It can be observed that the electrostatic contribution is the largest followed by charge transfer and polarization for all the structures. The EDA of the other complexes shows that the contribution from the electrostatic term is always greater than the others. EDA analysis thus gives justification for the use of the electrostatic model for the investigation of carbonyl···HF complexes.

BSSE and ZPE Correction. Table 4 presents the BSSE- and ZPE-corrected intermolecular interaction energies. BSSE energy is calculated using eq 6, which can be simplified to $E_{BSSE} = E_{FCPE} - E_{FRE}$, where E_{FCPE} and E_{FRE} are the function counterpoise and fragment relaxation energy corrections, respectively. The energy ranking of the structures remains the same upon total correction except for the halogen-substituted complexes. It can be seen from Table 4 that the E_{FCPE}, E_{FRE}, and E_{ZPE} are nearly equal for the entire series of carbonyl molecules, which is in agreement with the earlier study.[21] However, substantial corrections are noted for the relatively weaker structures, e.g., structure **1** of Cl-, CN-, and CF_3-substituted complexes. Total correction due to BSSE and ZPE is found to be 20−40% of the ΔE_{SCF}.

IV. Concluding Remarks

This work has clearly indicated that the strength of MESP at the CP's of carbonyl molecules can be employed for predicting the sites of HF binding as well as the respective binding energies. It is observed that HF does not always bind from the nonsubstituted side of carbonyl molecule, as reported by Bobadova-Parvanova and Galabov.[21] For instance, if the hydroxyl or amine group is attached, then the binding is more favorable from the substituted side. For all the complexes, it is found that the initial site predicted by the EPIC model is very close to the final optimized one.

In this work, we have employed the split valence polarized Gaussian (6-31G**) basis set. In an earlier study,[32a] it is found that the MESP topographical features are sufficiently well-reproduced at this basis set. Further, it has been shown[32b] that the incorporation of electron correlation does not alter the CP characteristics at this level of basis. Our earlier investigation[33] has also concluded that the inclusions of diffuse basis functions in the above basis (6-31++G(d,p)) do not change the energy ranking of the structures of the hydrogen-bonded complexes.

To explore the role of correlation for these complexes, a study including correlation (MP2/ 6-31G** basis level) is carried for the HCHO···HF complex as a test case. It is observed that the interaction energy values for structures **1** and **3** are −41.65 and −27.44 kJ mol^{-1}, indicating an enhancement of 5−6 kJ mol^{-1}. However, the energy ranking of the structures is not altered by the MP2 method. Similarly, the basis set superposition error (BSSE) and ZPE calculations are carried out for the entire series of complexes. Total correction due to them is about 40% of the SCF interaction energy.

In a recent work,[17,33] we have carried out the Kitaura-Morokuma[31] interaction energy decomposition analysis for similar types of complexes, viz. C_3H_6···NH_3 and C_3H_8···NH_3. The analysis shows that the electrostatic component is dominant over the charge transfer, polarization, and exchange terms of the energy. With some experience in handling such complexes,

TABLE 4: BSSE and Zero-Point Energy (E_{ZPE}) Corrections in the ab Initio Intermolecular Interaction Energy (ΔE_{SCF}) for Structures 1 and 2 (See Figure 1)[a]

	structure **1**						structure **2**					
complex	ΔE_{SCF}	E_{FCPE}	E_{FRE}	E_{BSSE}	E_{ZPE}	ΔE_{SCFBZ}	ΔE_{SCF}	E_{FCPE}	E_{FRE}	E_{BSSE}	E_{ZPE}	ΔE_{SCFBZ}
HCHO···HF	−3.82	−8.33	0.14	−8.47	10.55	−14.79	−33.82	−8.33	0.14	−8.47	10.15	−14.79
HCOF···HF	−27.94	−8.73	0.63	−9.36	8.38	−10.23	−24.09	−2.88	0.47	−3.35	7.18	−13.56
HCOCl···HF	−25.93	−8.81	0.67	−9.48	8.03	−8.42	−21.13	−2.47	0.58	−3.04	6.84	−11.25
HCOOH···HF	−49.15	−11.91	2.16	−14.07	11.33	−23.75	−35.14	−8.32	0.99	−9.32	9.36	−16.46
HCOSH···HF	−36.34	−10.19	1.19	−11.39	10.01	−14.94	−32.18	−8.42	0.86	−9.28	9.05	−13.85
HCOCN···HF	−26.26	−9.58	0.30	−9.94	8.19	−8.13	−17.69	−8.39	0.23	−8.63	6.34	−2.27
$HCONH_2$···HF	−54.99	−11.49	2.36	−13.85	12.88	−28.26	−45.79	−8.36	1.62	−9.98	11.18	−24.63
$HCOCH_3$···HF	−39.90	−9.62	0.84	−10.46	10.13	−21.23	−37.94	−8.35	0.82	−9.17	9.71	−19.06
$HCOCF_3$···HF	−27.09	−9.61	1.31	−10.93	8.21	−9.36	−21.48	−3.50	0.54	−4.03	6.65	−10.43
$HCONO_2$···HF	−29.26	−9.09	0.43	−9.52	7.47	−10.86	−21.40	−4.09	0.31	−4.40	6.33	−11.03

[a] Individual terms are defined in Methodology. E_{FCPE} and E_{FRE} denote the function counterpoise and fragment relaxation energy corrections, respectively. Total BSSE error: $E_{BSSE} = E_{FCPE} - E_{FRE}$. Total interaction energy: $\Delta E_{SCFBZ} = \Delta E_{SCF} - E_{BSSE} + E_{ZPE}$. Energies are in kJ mol^{-1}.

we believe that these trends are generally valid for the present work as well. This analysis and the aforementioned success of electrostatic-based models indicate that such models can be fruitfully applied to the study of rather weakly bound complexes.

The directionality of approach of the HF molecule is found to depend on the substituent group. For instance, the F atom in HF is seen to repel away from the electronegative substituent. Similarly, if the acidic proton is attached to C═O, then the F end of HF tilts toward the proton.

Attachment of the electron-withdrawing group makes the MESP value at CP numerically smaller, resulting in a smaller interaction energy. An electron-donating group exactly does the reverse and enhances the value of the interaction energy. A remarkable plot of ab initio interaction energy versus EPIC model energy (cf. Figure 2) indeed brings out the utility of the EPIC model toward such a study.

With this qualitative and quantitative predictive ability and simplicity of approach, it is felt that EPIC model would be highly useful for studying interaction energies of the complexes formed by large molecules. Such applications are currently being explored in our laboratory.

Acknowledgment. Thanks are due to the Council of Scientific and Industrial Research (CSIR) [01(1430)/96/EMR-II], New Delhi, for providing financial support and to the Center for Development of Advanced Computing (C-DAC), Pune, for making available the computational resources.

References and Notes

(1) (a) Leszczynski, J., Ed. *Computational Chemistry*; World Scientific: River Edge, NJ, 1996. (b) Jeffrey, G. A.; Saenger, W. *Hydrogen Bonding in Biological Structures*; Springer-Verlag: Berlin, 1991.

(2) French, A. D.; Miller, D. P. In *Modeling the Hydrogen Bond*; Smith, D. A., Ed.; American Chemical Society: Washington, DC, 1994; Chapter 15.

(3) Remko, M.; Scheiner, S. *J. Pharm. Sci.* **1991**, *80*, 328.

(4) Pauling, L. *The Nature of the Chemical Bond*, 3rd ed.; Cornell University Press: Ithaca, NY, 1960; p 331.

(5) Baiocchi, F. A.; Klemperer, W. *J. Chem. Phys.* **1983**, *78*, 3509.

(6) (a) Florian, J.; Johnson, B. G. *J. Phys. Chem.* **1995**, *99*, 5899. (b) Field, M. J.; Bash, P. A.; Karplus, M. *J. Comput. Chem.* **1990**, *11*, 700. (c) Lavas, F. J.; Suenram, R. D.; Fraser, G. T.; Gillies, C. W.; Zozom, J. *J. Chem. Phys.* **1987**, *88*, 722. (d) Neuheuser, T.; Hess, B. A.; Reutel, C.; Weber, E. *J. Phys. Chem.* **1994**, *98*, 6459. (e) Gao, J. In *Modeling the Hydrogen Bond*; Smith, D. A., Ed.; American Chemical Society: Washington, DC, 1994; Chapter 2.

(7) (a) Turi, L. *J. Phys. Chem.* **1996**, *100*, 11285. (b) Harmony, M. D.; Laurie, V. W.; Schwendeman, R. H.; Ramsay, D. A.; Lovas, F. J.; Lafferty, W. J.; Maki, A. G. *J. Phys. Chem.* **1979**, *8*, 619. (c) Wiechert, D.; Mootz, D.; Dahlems, T. *J. Am. Chem. Soc.* **1997**, *119*, 12665. (d) Qian, W.; Krimm, S. *J. Phys. Chem. A* **1998**, *102*, 659.

(8) Legon, A. C.; Millen, D. J. *Chem. Soc. Rev.* **1987**, *16*, 467. (b) Crabtree, R. H. *Chem. Rev.* **1995**, *95*, 987. (c) Andrews, A. M.; Hilling, K. W., II; Kuczkowski, R. L. *J. Am. Chem. Soc.* **1992**, *114*, 6765.

(9) Hobza, P.; Zahradnik, R. *Chem. Rev.* **1988**, *88*, 871.

(10) (a) Buckingham, A. D.; Fowler, P. W. *Can. J. Chem.* **1985**, *63*, 2018. (b) Buckingham, A. D.; Fowler, P. W. *J. Chem. Phys.* **1983**, *79*, 6426.

(11) (a) Dykstra, C. E. *J. Am. Chem. Soc.* **1989**, *111*, 6168. (b) Alhambra, C.; Luque, F. J.; Orozco, M. *J. Phys. Chem.* **1995**, *99*, 3084.

(12) (a) Politzer, P. In *Chemical Applications of Atomic and Molecular Potentials*; Politzer, P., Truhlar, D. G., Eds.; Plenum: New York, 1981; Chapter 2. (b) Scrocco, E.; Tomasi, J. *Topics in Current Chemistry*; Springer: Berlin, 1973; p 42. (c) Bonaccorsi, R.; Scrocco, E.; Tomasi, J. *J. Chem. Phys.* **1970**, *52*, 5270.

(13) (a) Murray, J. S.; Lane, P.; Brinck, T.; Paulsel, K.; Grice, M. E.; Politzer, P. *J. Phys. Chem.* **1993**, *97*, 9369. (b) Politzer, P.; Seminario, J. M. *J. Phys. Chem.* **1989**, *93*, 4742.

(14) Náray-Szabo, G.; Ferenczy, G. G. *Chem. Rev.* **1995**, *95*, 829.

(15) Haeberlein, M.; Brinck, T. *J. Phys. Chem.* **1996**, *100*, 10116.

(16) Gadre, S. R.; Suresh, C. H. *J. Org. Chem.* **1997**, *62*, 2625.

(17) Gadre, S. R.; Pingale, S. S. *J. Am. Chem. Soc.* **1998**, *120*, 7056.

(18) Gadre, S. R.; Bhadane, P. K.; Pundlik, S. S.; Pingale, S. S. In *Molecular Electrostatic Potentials: Theory and Applications*; Murray, J. S., Sen, K. D., Eds.; Elsevier: Amsterdam, 1996; p 219.

(19) Gadre, S. R.; Pundlik, S. S. *J. Phys. Chem. B* **1997**, *101*, 3298.

(20) Pundlik, S. S.; Gadre, S. R. *J. Phys. Chem. B* **1997**, *101*, 9657.

(21) Bobadova-Parvanova, P.; Galabov, B. *J. Phys. Chem. A* **1998**, *102*, 1815.

(22) Tomasi, J.; Bonaccorsi, R.; Cammi, R. In *Theoretical Methods of Chemical Bonding*; Maksic, Z. B., Ed.; Springer: Berlin, 1990; Vol. 3.

(23) (a) Gadre, S. R.; Shrivastava, I. H. *J. Chem. Phys.* **1991**, *94*, 4384. (b) Gadre, S. R.; Kölmel, C.; Ehrig, M.; Ahlrichs, R. *Z. Naturforsch.* **1993**, *48a*, 145.

(24) For details, see the following. Bader, R. F. W. *Atoms in Molecules, A Quantum Theory*; Clarendon Press: Oxford, 1990.

(25) Boys, S. F.; Bernardi, F. *Mol. Phys.* **1970**, *19*, 553.

(26) Xantheas, S. S. *J. Chem. Phys.* **1996**, *104*, 8821.

(27) Schmidt, M. W.; Baldridge, K. K.; Boatz, J. A.; Elbert, S. T.; Gordon, M. S.; Jensen, J. J.; Koseki, S.; Matsunaga, N.; Nguyen, K. A.; Su, S.; Windus, T. L.; Dupuis, M.; Montgomery, J. A. GAMESS. *J. Comput. Chem.* **1993**, *14*, 1347.

(28) Limaye, A. C.; Gadre, S. R. *J. Chem. Phys.* **1994**, *100*, 1303.

(29) Shirsat, R. N.; Bapat, S. V.; Gadre, S. R. *Chem. Phys. Lett.* **1992**, *200*, 373.

(30) Chipot, C. *GRID: The FORTRAN program for fitting charges to molecular electrostatic potentials and fields*; University de Nancy I: France, 1992.

(31) (a) Kitaura, K.; Morokuma, K. *Int. J. Quantum Chem.* **1976**, *10*, 325. (b) Morokuma, K.; Kitaura, K. In *Chemical Applications of Electrostatic Potentials*; Politzer, P., Truhlar, D. G., Eds.; Plenum: New York, 1981.

(32) (a) Gadre, S. R.; Kulkarni, S. A.; Suresh, C. H.; Shrivastava, I. H. *Chem. Phys. Lett.* **1994**, *239*, 273. (b) Kulkarni, S. A. *Chem. Phys. Lett.* **1996**, *254*, 268.

(33) Gadre, S. R.; Bhadane, P. K. *Theor. Chem. Acc.* **1998**, *100*, 300.